Nano

Volume: 11, Number: 03 (March 2016)

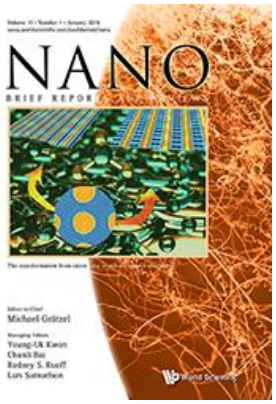

BRIEF REPORTS

1. The Meyer–Neldel Rule in Conduction Mechanism of the Electrospun ZnO Nanofibers

Andrzej Stafiniak, *Marek Tłaczała*

1650025

In the current study, we showed that the behavior of ZnO nanofibers is consistent with the Meyer–Neldel rule. Compatibility of the experimental data with the Meyer–Neldel rule suggests exponential energy distribution of the deep level traps in the material. This allowed the development of improved conductivity model of a single electrospun ZnO nanofiber which well describes the nanofiber conductivity in oxide rich and neutral atmosphere.

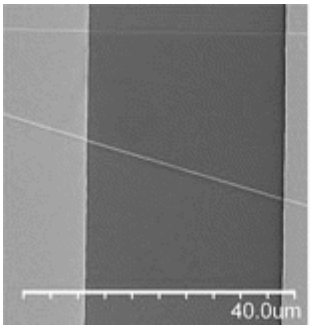

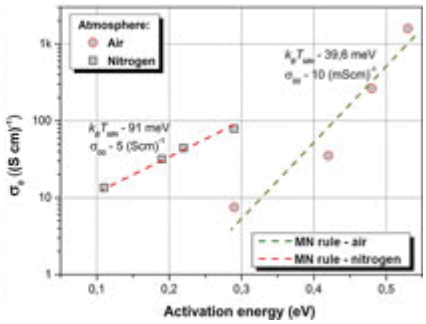

2. Deposition of Nd-Doped Fe_2O_3 Nanoparticles on Cenosphere by Hydrothermal Method

Hui Zhang, *Yuanyuan Shi*, *Jun Xu*, *Runjun Sun*

1650026

In the present study, we fabricated the Nd-doped Fe_2O_3-coated cenosphere by a simple hydrothermal method. The photoactivity and magnetic properties are improved to some extent by incorporating a small amount of rare earth Nd^{3+} ions. The concentration of Nd^{3+} ions is optimized to be 0.4% in relation to Fe^{3+} for the photocatalytic degradation of methylene blue dye. The Nd element is dispersed on the surface of Nd-doped Fe_2O_3 nanoparticle in the form of Nd_2O_3 nanocrystallites.

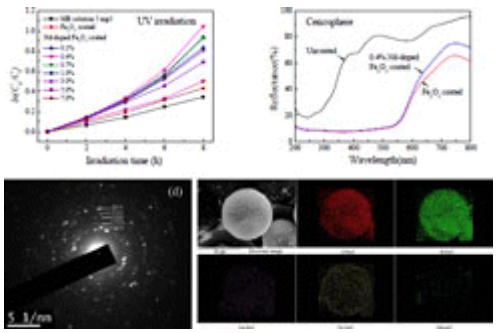

3. Small-Angle X-Ray Scattering Study on PVA/Fe_3O_4 Magnetic Hydrogels

Sunaryono, *Ahmad Taufiq*, *Edy Giri Rahman Putra*, *Atsushi Okazawa*, *Isao Watanabe*, *Norimichi Kojima*, *Supagorn Rugmai*, *Siriwat Soontaranon*, *Mohammad Zainuri*, *Triwikantoro*, *Suminar Pratapa*, *Darminto*

1650027

The PVA/Fe_3O_4 magnetic hydrogels were successfully fabricated by freezing-thawing processes. The structures were investigated by using small angle X-ray scattering. The secondary particles and clusters of magnetite nanoparticles in the magnetic hydrogels fitted by two lognormal distributions presented clustering degradation with lowering Fe_3O_4composition. Furthermore, the effect of clustering on the magnetic properties was also performed by means of SQUID magnetometer. The saturation magnetization of the magnetic hydrogels is proportional to the Fe_3O_4composition and also their clusters.

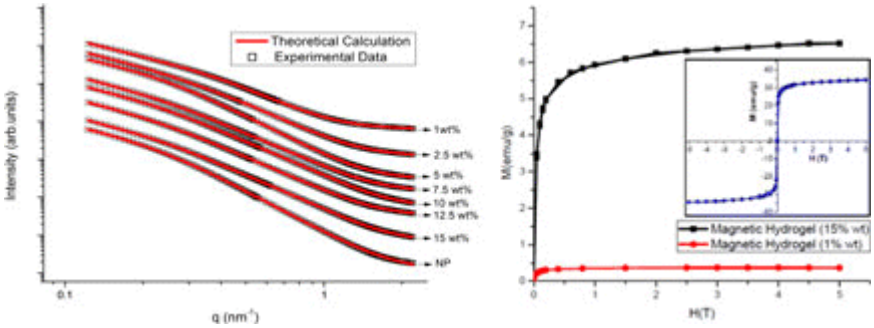

4. Preparation of N-Doped Nanoporous Carbon from Crude Biomass and its Electrochemical Activity

Zezhong Xu, *Jingyu Si*

1650028

N-doped nanoporous carbons with high surface area were prepared from the highly available, accessible and recyclable plant, Typha orientalis. The linearity between H_2O_2 concentration and the responding current signal proved the potential of N-doped nanoporous carbon to be applied in electrochemical sensing. The obtained products may have further use for glucose biosensing.

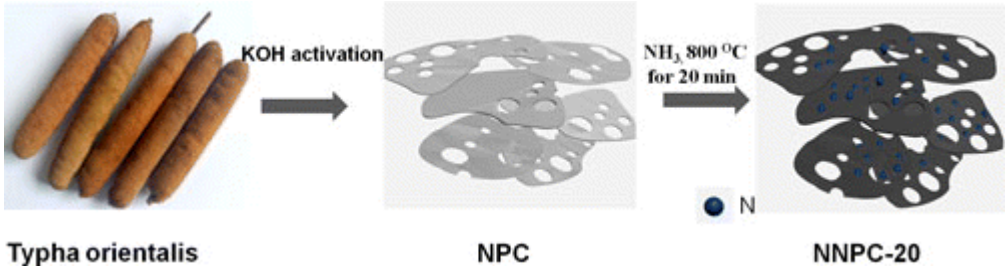

5. **Effects of Temperature and Hydrogen-Like Impurity on the Vibrational Frequency of the Polaron in RbCl Parabolic Quantum Dots**

Wei Xiao, Jing-Lin Xiao

1650029

The effects of temperature and hydrogen-like impurity on the vibrational frequency of the polaron in RbCl parabolic quantum dots have been studied. The linear combination operator method, unitary transformation and the quantum statistics theory methods have also been explored and the expressions for the strong-coupling polaron's vibrational frequency, ground state energy and the ground state binding energy were derived.

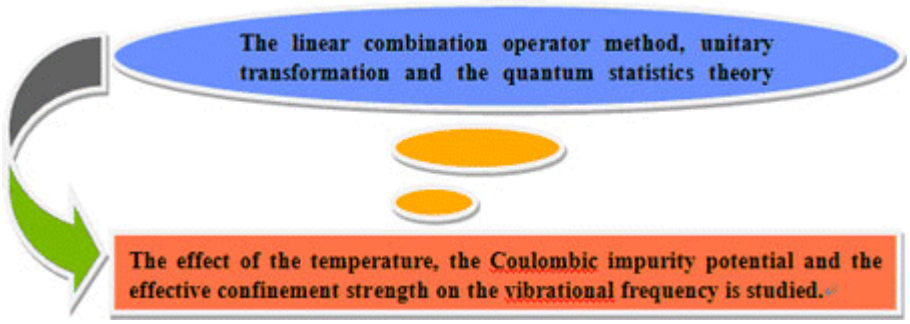

6. **Epitaxial Growth of Strain-Induced Ferromagnetic $LaCoO_3$ Thin Films by Simple Sol–Gel Technique**

Haifeng Liu, Yuqiao Guo, Ruishi Xie, Guohua Ma

1650030

$LaCoO^3$ epitaxial thin films with good crystalline property were successfully grown on (001) oriented $LaAlO^3$substrates by the simple sol–gel technique. Different from the nonmagnetic ground state of polycrystalline $LaCoO^3$, an obvious ferromagnetic transition at TC∼85 K was observed in $LaCoO^3$ epitaxial film. The strain-induced ferromagnetism originates from an increase of the Co–O bond length and a suppression of the CoO^6 octahedral rotations, which stabilizes higher spin state of Co^{3+} by a decrease of eg−t2geg−t2g gap energy.

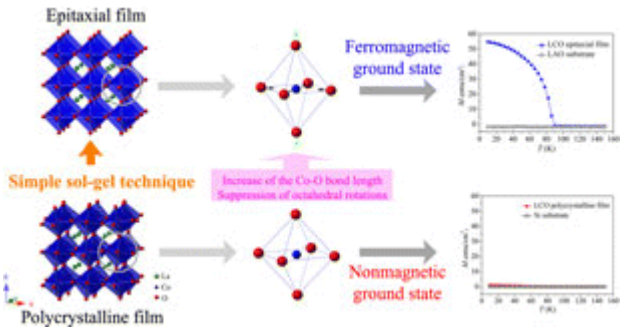

7. **A Low-Cost Nano/Micro Structured-Silicon-MWCNTs from Nano-Silica for Lithium Storage**

Xuejiao Feng, *Tengda Ding*, *Hongmin Cui*, *Nanfu Yan*, *Fei Wang*

1650031

A low-cost nano/microstructure of Si-CNT was derived from nano-SiO_2 and multiwall carbon nanotubes through spray drying, and followed by the reduction of silica-MWCNTs magnesiothermic reaction in the presence of NaCl as a heat scavenger. Si nanoparticles were directly deposited on the surface of the MWCNT and possessed a good contact between Si and MWCNTs, connecting and reinforcing the whole structure. Comparing to ball milling, a combination of SiO_2, MWCNTs and NaCl by spray drying achieved long cycle life for Si-CNT composite.

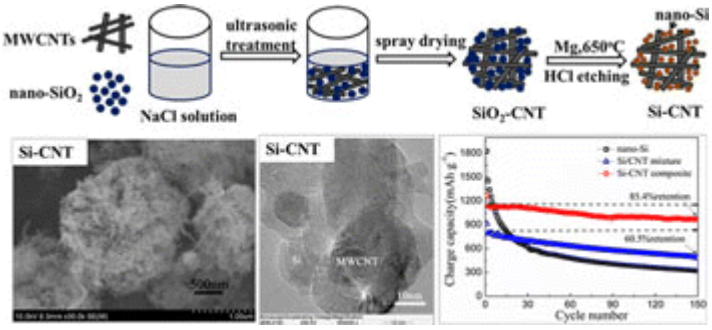

8. **Synthesis of Novel Hollow Copper Oxide Micro-Flowers Assembled by Nanoparticles and Their Improved Catalytic Performances for the Synthesis of Organosilane**

Hongwei Che, *Aifeng Liu*, *Jingbo Mu*, *Xiaoliang Zhang*

1650032

Used as the catalysts for the synthesis of organosilane, novel sisal-like hollow CuO micro-flowers assembled by nanoparticles exhibit better catalytic performances than the commercial CuO powders due to their hollow and flower-like structures.

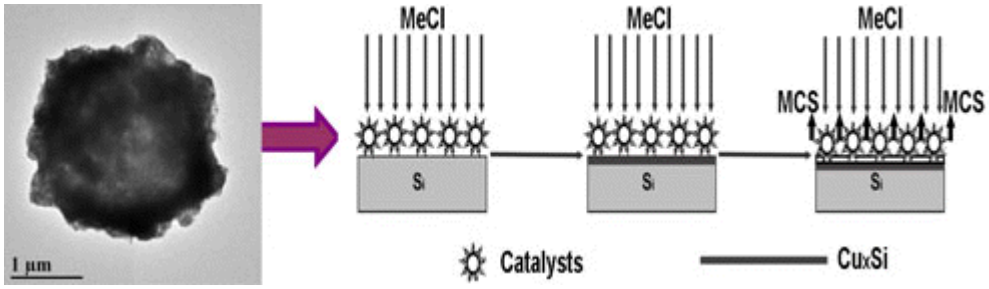

9. Synthesis and Optical Limiting Properties of Graphene Oxide/Bimetallic Nanoparticles

Shuguang Cai, *Chan Zheng*, *Xueqing Xiao*, *Xiaoyun Ye*

1650033

Pt and Cu NPs were simultaneously deposited on graphene oxide (GO) sheets by the hydrothermal reaction. Their nonlinear optical (NLO) and optical limiting (OL) properties were characterized by open-aperture Z-scan measurements. The GO/bimetallic NPs exhibited enhanced NLO and OL properties. The two-photon absorption, nonlinear scattering, inter-band transition, and charge transfer contributed to the enhanced NLO and OL properties of the GO/Pt-Cu NPs.

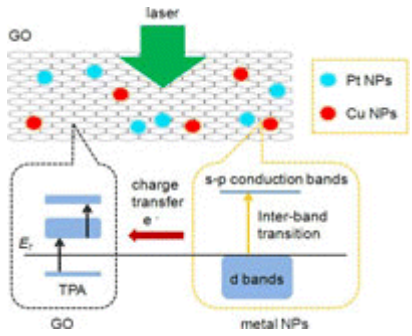

10. Anomalous Ferromagnetism and Electron Microscopy Characterization of High-Quality Neodymium Oxychlorides Nanocrystals

Xinliang Zheng, *Juan Feng*, *Jiarui Zhang*, *Hongna Xing*, *Jiming Zheng*, *Mingzi Wang*, *Yan Zong*, *Jintao Bai*, *Xinghua Li*

1650034

In the current study, well-defined NdOCl nanocubes with tetragonal PbFCl matlockite phase were fabricated through a non-hydrolytic thermolysis route. Magnetic measurement suggested that the NdOCl nanocubes reveal abnormal ferromagnetic characteristic at room temperature, which is quite different from the corresponding antiferromagnetic bulk. These results are believed to be significant for the field of diluted magnetic semiconductors and rare earth-based nanostructures.

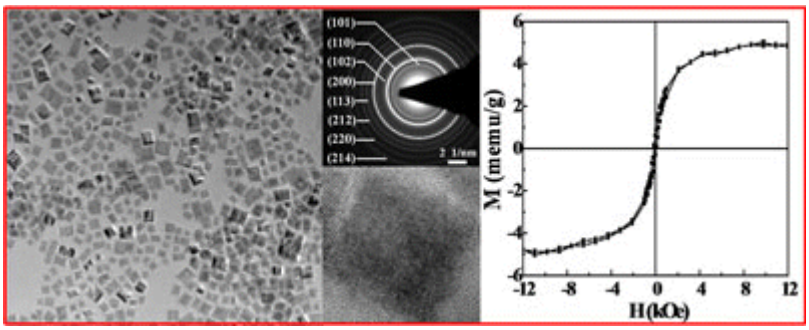

11. One-Pot Hydrothermal Synthesis of Sulfur-Doped SnO_2 Nanoparticles and their Enhanced Photocatalytic Properties

Lin Ma, *Limei Xu*, *Xuyao Xu*, *Xiaoping Zhou*, *Lingling Zhang*

1650035

Ultrafine sulfur-doped SnO_2 nanoparticles are prepared by a one-pot hydrothermal method. The doping level of sulfur element as well as the bandgaps of SnO_2 can be controlled, to a certain extent. The resultant sulfur-doped SnO_2 nanoparticles demonstrate obvious enhanced photocatalytic activities due to effective separation of the photo-generated electron–hole pairs.

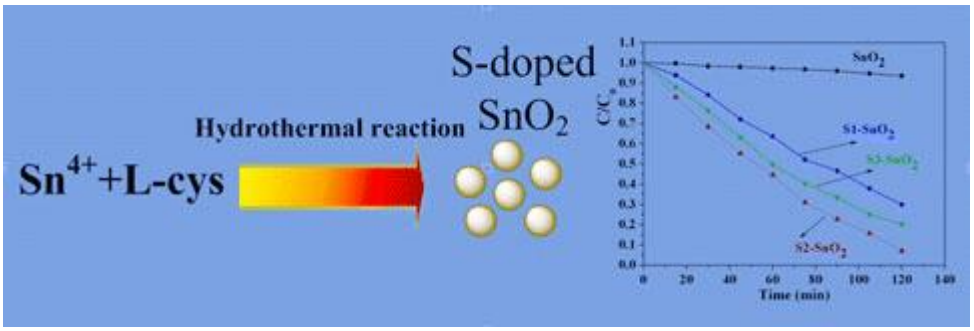

12. Molybdenum Trioxide Dihydrate-Graphene Composite for Electrochemical Detection of Thiourea Molecule

Xinmeng Zhang, *Kezhi Li*, *Hejun Li*, *Jinhua Lu*, *Leilei Zhang*

1650036

Molybdenum trioxide dihydrate ($MoO3{\cdot}23{\cdot}2H_2O$)-graphene composite was synthesized by a selfassembly procedure and was used to modify electrode for fabrication of novel sensitive electrochemical sensor. This sensor has excellent electrochemical properties for the detection of thiourea, which are attributed to the loose porous structure of composite and the synergistic effects between graphene and $MoO3{\cdot}23{\cdot}2H_2O$.